Dalton Transactions

Accepted Manuscript

ROYAL SOCIETY OF CHEMISTRY

www.rsc.org/dalton

Journal Name

RSCPublishing

ARTICLE

Cite this: DOI: 10.1039/x0xx00000x

Received ooth January 2012,
Accepted ooth January 2012

DOI: 10.1039/x0xx00000x

www.rsc.org/

Neutral N^C^N terdentate luminescent Pt(II) complexes: synthesis, photophysical properties and bio-imaging application

Alessia Colombo,[a#] Federica Fiorini,[b#] Dedy Septiadi,[b#] Claudia Dragonetti,[a,c,*] Filippo Nisic,[a] Adriana Valore,[a] Dominique Roberto,[a,c] Matteo Mauro,[b,d,*] Luisa De Cola[b,*]

An emerging field regarding N^C^N terdentate Pt(II) complexes is their application as luminescent labels for bio-imaging. In fact, phosphorescent Pt complexes display many advantages such as wide emission color tunability, better stability towards photo- and chemical degradation, very large Stokes shift, long-lived luminescent excited states with lifetimes typically two to three orders of magnitude longer than those of classic organic fluorophores. Here, we describe the synthesis and photophysical characterization of three new neutral N^C^N terdentate cyclometallated Pt complexes as long-lived bio-imaging probes. The novel molecular probes bear hydrophilic (oligo-)ethylenglycol chains of various length in order to increase their water solubility, bio-compatibility and impart amphiphilic nature to the molecules. The complexes are characterized by a high cell permeability and low cytotoxicity, with an internalization kinetics that depends on both the length of the ethylenglycol chain and the ancillary ligand.

Introduction

The discovery of cisplatin $\{PtCl_2(NH_3)_2\}$ anticancer activity[1] and its following important clinical success have lead to an increasing interest in the development of platinum-based drugs.[2-5] In addition, d^8 platinum(II) complexes have attracted much attention due to their interesting luminescent properties.[6-10] Cyclometallated derivatives are usefully employed for the preparation of triplet emitters for highly efficient OLED (organic light emitting diode) devices[7,11-14] and for their appealing second-order nonlinear optical (NLO) properties.[15-18]

Another fast emerging field regarding luminescent Pt(II) complexes is their application as luminescent labels for bio-imaging.[19-23] Although fluorescent organic labels are still the leading choice for such applications,[24-26] phosphorescent Pt(II) complexes are slowly getting attention and could outclass organic molecules. In fact, Pt complexes display many advantages such as: (i) a wide emission colour tunability by an adequate choice of the ligands; (ii) a better stability towards photo- and chemical degradation; (iii) very large Stokes shift that allows the detection of their emission at a much lower energy than the excitation energy; (iv) long-lived luminescent excited states owing to their triplet-manifold nature; (v) emission lifetimes typically two to three orders of magnitude longer than those of classic organic fluorophores. Another important point is related to synthetic issues: modification of many fluorescent organic structures can be difficult and laborious, whereas Pt complexes can be prepared using well-defined and faster strategies, often involving stepwise introduction of different ligands. One argument sometimes raised against the use of platinum is its high cost. However, for bio-imaging application, the amount of material requested is minimal and the cost of the metal is often only a relatively minor fraction of the total synthetic efforts.

Nonetheless, it is worth pointing out that UV light might damage biological specimens and that tissues are relatively transparent at wavelengths in the range 600–1300 nm, called the optical therapeutic window. Furhermore, red and near infra-red (NIR) light is highly desirable for both excitation and detection due to the lack of overlap with auto-fluorescence of biomolecules and the larger penetration of photons with such spectral energy. For these reasons, molecules displaying relatively high two-photon absorption cross-section into the NIR are good candidates, and in this respect platinum complexes could be key players.[20,22]

The investigation of platinum complexes for biological applications concerns mostly monomeric compounds, but aggregates show some important features as well:[19,20] i) the emitter is shielded from the environment and in particular from dioxygen that could induce quenching; ii) the rigidity, due to the packing of molecules in determined structures, decreases non-radiative processes; iii) the reactivity or toxicity of the complexes is diminished by the difficult accessibility of the metal centre; iv) changes in the excited state nature and properties lead to a bathochromic shift of excitation and emission towards more biologically interesting spectral windows and sometimes to an enhancement of the photophysical properties.

In this respect, amongst all luminescent platinum derivatives, those bearing either an N^C^N[22,23] or, more recently, an N^N^N[19,20,27] chromophoric ligand have shown very interesting results. Although the growing interest and the emerging potential application as bio-imaging and/or theragnostic agents that luminescent platinum complexes possess, a chemical structure – internalization relationship remains still a challenging and rather elusive goal to date.[20,28,29]

To this purpose, we decided to undertake a systematic study of the bio-imaging and cytotoxicity features for a series of platinum complexes bearing a N^C^N cyclometallated 1,3-di(2-pyridyl)-benzene, varying the molecular hydrophobic/hydrophilic ratio (through the introduction of ethylenglycol moieties of different length) and the ancillary ligand, the incubating media and the staining concentration. The choice of oligo-ethyleneglycol chains on the phosphorescent probe was based on their known ability to increase the aqueous solubility and bio-compatibility of luminescent iridium bio-labels.[30]

In the present work, we thus describe the synthesis and photophysical characterization of three new neutral terdentate N^C^N cyclometallated Pt complexes (Figure 1) as long-lived bio-imaging probes. As it will be hereafter discussed, the novel complexes bear hydrophilic moieties and they are characterized by a high cell permeability and low cytotoxicity, with an internalization kinetics that depends on both the ethylenglycol chain length and the ancillary ligand.

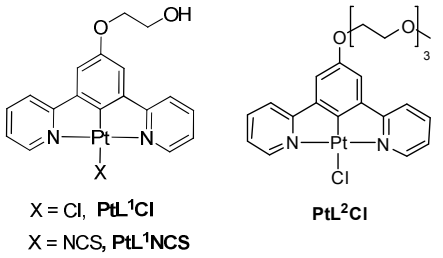

Figure 1. Chemical structure of the investigated neutral platinum complexes.

Experimental

General comments

Solvents were dried by standard procedures: *N,N*-dimethylformamide (DMF) was dried over activated molecular sieves; toluene was distilled over Na/benzophenone. All reagents were purchased from Sigma-Aldrich and were used without further purification. Reactions requiring anhydrous conditions were performed under argon. ^{1}H NMR spectra were recorded at 400 MHz on a Bruker AVANCE-400 instrument. Chemical shifts (δ) for ^{1}H spectra are expressed in ppm relative to Me_4Si as the internal standard. Mass spectra were obtained with a FT-ICR Mass Spectrometer APEX II & Xmass software (Bruker Daltonics) - 4.7 Magnet and Autospec Fission Spectrometer (FAB ionization). Thin layer chromatography (TLC) was carried out with pre-coated Merck F_{254} silica gel plates. Flash chromatography (FC) was carried out with Macherey-Nagel silica gel 60 (230–400 mesh). The schematic synthetic pathway employed for the preparation of the reported platinum complexes is displayed in Scheme 1.

Synthesis of compound 1

Under argon atmosphere, 2-hydroxyethyl tosylate (1.02 g, 4.70 mmol) was added to a solution of 3,5-dibromophenol (800 mg, 3.17 mmol) and K_2CO_3 (8.372 mg, 6.84 mmol) in 17.6 mL of dry DMF. The mixture was stirred at 90°C overnight. The reaction mixture was diluted with ethyl acetate (100 mL), washed with water (150 mL) and brine (100 mL), then the organic layer was dried over Na_2SO_4 and the solvent removed under reduced pressure. The obtained crude product was purified by flash chromatography on silica gel using hexane:ethyl acetate 4:1 as eluent, to give 798 mg of product (85% yield).
^{1}H NMR (400 MHz, CD_2Cl_2): δ 7.30 (s, 1H), 7.06 (s, 1H), 7.04 (s, 1H), 4.1 (m, 2H), 3.95 (m, 2H). Elemental Analysis: Calcd. for $C_8H_8Br_2O_2$: C, 32.47; H, 2.72. Found: C, 32.40; H, 2.80.

Synthesis of compound 2

A mixture of 3,5-dibromophenol (592 mg, 2.35 mmol), 2-(tri-*n*-butylstannyl)pyridine (1.83 mL 5.65 mmol), $PdCl_2(PPh_3)_2$ (100 mg, 0.14 mmol), and LiCl (1.8 g, 42.5 mmol) was suspended in 6 mL of degassed toluene, and heated under reflux for 48 hours. After cooling down to room temperature, aqueous NaOH (1M, 30 mL) was added. The phases were separated and the aqueous phase was extracted with ethyl acetate (3 × 100 mL).
The combined organic layers were dried over Na_2SO_4 and concentrated in *vacuo*. The crude product was purified by flash chromatography on silica gel (ethyl acetate:hexane 7:3). The product was isolated as pale yellow oil in 60% yield.
^{1}H NMR (400 MHz, $CDCl_3$): δ 8.71 (d, J = 4.64 Hz, 2H), 8.18 (s, 1H), 7.82 -7.75 (m, 2H), 7.63 (s, 2H), 7.44 (d, J = 4.64 Hz, 2H), 7.31 (m, 2H). Elemental Analysis: Calcd. for $C_{16}H_{12}N_2O$: C, 77.40; H, 4.87; N, 11.28. Found: C, 77.38; H, 4.85; N, 11.33. MS(FAB+): m/z 248.

Synthesis of the pro-ligand HL^1

Under a nitrogen atmosphere, a mixture of the 5-substituted *m*-dibromobenzene derivative **1** (150 mg, 0.51 mmol), 2-(tri-n-butylstannyl)pyridine (495 μL 1.53 mmol), $PdCl_2(PPh_3)_2$ (35.8 mg, 0.051 mmol), CuO (124 mg, 1.53 mmol) and DMF (2 mL) was placed in a microwave reactor at 160 °C (250 W) for 45 min, controlling the flow rate of cooling air. After cooling to room temperature, the reaction mixture was poured into ethyl acetate (25 mL) and filtered. The filtrate was washed with water, the organic layer was dried over anhydrous Na_2SO_4 and concentrated under reduced pressure. The crude product was purified by flash chromatography, using hexane:ethyl acetate 1:9 as the eluent. Yield 62%.
^{1}H NMR (400 MHz, $CDCl_3$): δ 8.72 (d, *J* =4.64 Hz, 2H), 8.20 (s, 1H), 7.83 (d, *J* =7.20 Hz, 2H), 7.78 (d, *J* =7.20 Hz, 2H), 7.67 (s, 2H), 7.27 (t, *J* =4.64 Hz, 2H), 4.30 (m, 2H) 4.03 (m, 2H).

Synthesis of the pro-ligand HL^2

A mixture of the intermediate **2** (50 mg, 0.2 mmol), tosylate derivative (96 mg, 0.3 mmol) and K_2CO_3 (55 mg, 0.4 mmol) in dry DMF (1 mL) under argon was heated at 90°C for 18 h. After cooling to room temperature the mixture was washed with 2 mL of pentane in order to remove the unreacted tosylate and then 3 mL of diethyl ether were added, the precipitate was filtered, and the yellow solution containing the pure ligand was dried under reduced pressure. The product was used without further purification.
^{1}H NMR (400 MHz, CD_2Cl_2): δ 8.71 (d, *J* = 4.6 Hz, 2H), 8.22 (s, 1H), 7.78 (d, *J* = 8.1 Hz, 2H), 7.77 (t, *J* = 8.1, 2H), 7.68 (s,

2H), 7.26 (t, *J* = 4.6 Hz, 2H), 4.34 (t, *J* = 4.0 Hz, 2H), 3.93 (t, *J* = 4.0 Hz, 2H), 3.80-3.78 (m, 2H), 3.72-3.63 (m, 4H, 3.57-3.55 (m, 2H), 3.38 (s, 3H). Elemental Analysis: Calcd. for $C_{23}H_{26}N_2O_4$: C, 70.03; H, 6.64; N, 7.10. Found: C, 69.98; H, 6.69; N, 7.15. MS(FAB+): m/z 395 [PtL^1].

Procedure for the synthesis of PtL^1Cl and PtL^2Cl

Under nitrogen atmosphere, a solution of K_2PtCl_4 (1 equiv.) and HL^1 or HL^2 (1 equiv.) in a AcOH:H_2O 9:1 mixture (0.3 M) was placed in a microwave reactor at 160 °C (250 W) for 45 minutes controlling the flow rate of cooling air. After cooling to room temperature, the reaction mixture was filtered. The precipitate was washed successively with methanol, water, ethanol and diethyl ether.

PtL^1Cl: 150 mg, 80% yield ^{1}H NMR (400 MHz, CD_2Cl_2): δ 9.30 (d, *J* = 4.7 Hz, 2H), 8.00 (q, *J* = 7.8 Hz, 2H), 7.74 (d, *J* = 7.8 Hz, 2H), 7.36 (t, *J* =4.7 Hz, 2H) 7.22 (s, 1H), 7.12 (s, 1H), 4.30 (m, 2H) 4.03 (m, 2H).
Elemental Analysis: Calcd. for $C_{18}H_{15}ClN_2O_2Pt$: C, 41.43; H, 2.90; N, 5.37. Found: C, 41.39; H, 2.88; N, 5.39.
MS(FAB+): m/z 486 [PtL^1].

PtL^2Cl: 100 mg, 70**%** yield ^{1}H NMR (400 MHz, CD_2Cl_2): δ 9.26 (d, *J* = 4.7 Hz, 2H), 8.00 (t, *J* = 7.8 Hz, 2H), 7.70 (d, *J* = 7.8 Hz, 2H), 7.19 (s, 2H), 7.06 (s, 1H), 4.24 (t, *J* = 4.0 Hz, 2H), 3.90 (t, *J* = 4.0 Hz, 2H), 3.81-3.79 (m, 2H), 3.70-3.63 (m, 4H), 3.57-3.55 (m, 2H), 3.38 (s, 3H).
Elemental Analysis: Calcd. for $C_{23}H_{25}ClN_2O_4Pt$: C, 44.27; H, 4.04; N, 4.49. Found: C, 44.30; H, 4.07; N, 4.51.
MS(FAB+): m/z 623 [PtL^2Cl], 588 [PtL^2].

Synthesis of PtL^1NCS

A solution of PtL^1Cl (125 mg, 1 equiv.) in dichloromethane (300 mL) was treated with a solution of sodium thiocyanate (15.1 mg, 1.1 equiv.) in methanol (2 mL). After stirring at room temperature under nitrogen for 24 hours, the solution was filtered and the solvent evaporated to dryness affording the crude product that was washed first with methanol and then with ethanol.
^{1}H NMR (400 MHz, CD_2Cl_2): δ 8.80 (d, *J* = 4.9 Hz, 2H); 8.06 (q, J= 7.8, 2H); 7.74 (d, *J* = 7.8 Hz, 2H); 7.39 (m, 2H); 7.17 (m, 2H); 4.49 (m, 2H); 4.30 (m, 2H).
Elemental Analysis: Calcd. for $C_{19}H_{15}N_3O_2PtS$: C, 41.91; H, 2.78; N, 7.72. Found: C, 41.89; H, 2.79; N, 7.70.
MS(FAB+): m/z 486 [PtL^1].

Photophysical measurements

Absorption spectra were measured on a Shimadzu UV-3600 double-beam UV−vis−NIR spectrophotometer and baseline-corrected. Steady-state emission spectra were recorded on a Horiba Jobin-Yvon IBH FL-322 Fluorolog 3 spectrometer equipped with a 450 W xenon arc lamp, double-grating excitation, and emission monochromators (2.1 nm mm^{-1} of dispersion; 1200 grooves mm^{-1}) and a TBX-04 photomultiplier as detector. Emission and excitation spectra were corrected for source intensity (lamp and grating) and emission spectral response (detector and grating) by standard correction curves.

Time-resolved measurements were performed using either the time-correlated single-photon counting (TCSPC) electronics PicoHarp300 or the Multi Channel Scaling (MCS) electronics NanoHarp 250 of the PicoQuant FluoTime 300 (PicoQuant GmbH, Germany), equipped with a PDL 820 laser pulse driver. A pulsed laser diode LDH-P-C-405 (λ = 406 nm, pulse FWHM <70 ps, repetition rate 200 kHz–40 MHz) was used to excite the sample and mounted directly on the sample chamber at 90°. The photons were collected by a PMA-C-192 photomultiplier (PMT) single photon counting detector. The data were acquired by using the commercially available software EasyTau (PicoQuant GmbH, Germany), while data analysis was performed using the commercially available software FluoFit (PicoQuant GmbH, Germany). For multi-exponential decays, the intensity, namely I(t), has been asumed to decay as the sum of individual single exponential decays:

$$I(t) = \sum_{i=1}^{N} \alpha_i \exp(-\frac{t}{\tau_i})$$

Excited state lifetimes values are given with ±10% relative uncertainty.
All the photoluminescence quantum yield measurements (PLQY) in solution were recorded at a fixed excitation wavelength (λ_{exc}= 400 nm) by using a Hamamatsu Photonics absolute PLQY measurement Quantaurus system equipped with continuous wave xenon light source (150 W), monochromator, integrating sphere, photonics multi-channel analyzer and employing the commercially available PLQY measurement software (Hamamatsu Photonics Ltd., Shizuoka, Japan). PLQY values are given with ±0.01 uncertainty.

Cell culture

All materials for cell culture were purchased from Gibco. *Human cervical carcinoma*, HeLa cells were cultured inside growing media containing 88% Dulbecco's Modified Eagle Medium (DMEM), 10% Fetal Bovine Serum (FBS), 1% Penicillin-Streptomycin and 1% L-Glutamine 200 mM under 37°C and 5% of CO_2 condition for 48 hours until reaching 80 to 85% cell confluency. Subsequently, the cells were washed twice with Phosphate Buffer Solution (PBS), trypsinated and approximately 50,000 cells were re-seeded on monolayer glass cover slip placed inside six-well plate culture dish and glass bottom dishes (MatTek). Fresh culture media (2 mL) was added gently and cells were grown overnight.

Platinum complexes incubation

The culture media was removed and 1 mL of staining solution containing the corresponding platinum complexes (50 μM in less than 1% DMSO containing PBS) were gently added onto the cells. After incubation at 37°C and 5% of CO_2 for 10 minutes, the staining medium was removed and the cell layer on glass cover slips was gently washed (three times) with PBS and fixed with 4% paraformaldehyde (PFA) solution for 10 min.

Organelle stainings

Cell layer was washed twice with PBS and rinsed in 0.1% Triton X-100 in PBS for 5 minutes and afterwards in 1% bovine serum albumin, BSA (Sigma Aldrich), in PBS for another 20 min. The cell layer on glass cover slip was stained with Phalloidin Alexa Fluor® 647 (Invitrogen), for *f*-actin/membrane staining for 20 min in the dark at room temperature, and washed twice with PBS. For nucleoli staining purpose, a 500 nM of SYTO® RNASelect™ Green Fluorescent Cell Stain (Invitrogen) solution was added onto cells for 20 minutes followed by PBS washing. For visualizing nuclear region, cell nucleus was stained with 4',6-diamidino-2-

phenylindole carboxamidine (DAPI) and washed twice with PBS. The cover slips were mounted onto glass slides for microscopy measurements.

Fluorescence confocal microscopy

Reported fluorescence images were taken by using Zeiss LSM 710 confocal microscope set up with 63× magnification and numerical aperture (NA) 1.3 of Zeiss LCI Plan-NEOFLUAR water immersion objective lens (Zeiss GmbH, Germany). The samples were excited by continuous wave (cw) laser at 405 nm. The emission of the complexes was collected in the range from 500 to 720 nm. For co-localization experiments, the samples priorly co-stained with different dyes, DAPI (excitation/emission wavelength: 358 nm/461 nm), SYTO® RNASelect™ (excitation/emission wavelength: 490 nm/530 nm), and Alexa Fluor® 647 Phalloidin (excitation/emission wavelength: 650 nm/668 nm) were excited independently at 405, 488 and 633 nm, respectively. All image processing was performed by using ZEN software (Zeiss GmbH, Germany) and FigureJ plugin (IBMP, UniStra) inside imageJ (NIH). False colour images were adjusted to better distinguish different complexes and complexes from cellular organelles.

Kinetics of internalization of the complex

The culture media of live cells grown onto glass bottom dishes was removed and 1 mL of complex staining solution (5 μM in less than 1% DMSO containing PBS) was added. The cells were subsequently imaged by confocal microscopy setup for one minute acquisition time for a total duration of 30 minutes.

Cell viability studies

Cellular viability was measured by an automatic cell counter CASY® (Roche Innovatis AG). Approximately 50000 cells were grown in 2 mL of culture media inside six-well plates at 37°C, 5% CO_2 environment for 48 hours. Culture media was removed and replaced by one mL staining solution of complex **PtL^{1}Cl**, **PtL^{1}NCS**, and **PtL^{2}Cl** (50 μM in less than 1% DMSO in culture media). After 30 minutes of incubation, the staining solution was removed to eppendorf tubes and 0.5 mL of trypsin were added. To detach the cell from the surface of the plate, cells were incubated for 5 minutes in the same condition explained before. Subsequently, 0.5 mL of fresh culture media was added to neutralize trypsin. Cell suspensions together with first solutions collected were removed into eppendorf tube and mixed together. 100 μL of the cell suspension was dissolved in 10 mL of CASY ton solution and measurement was performed. Positive control of cells grown without complex was also added. All experiments were repeated at least three times.

Results and discussion

Synthesis

The proligands HL^1 and HL^2 were synthesized from the commercially available 3,5-dibromophenol and the appropriate hydrophilic chain activated as tosylate, prepared according to the literature[31] (Scheme 1). Complexes PtL^1Cl and PtL^2Cl were synthesized by reaction of K_2PtCl_4 with HL^1 and HL^2 respectively, in a $CH_3COOH–H_2O$ (9:1 v/v) mixture placed in a microwave reactor at 160°C for 45 minutes, as previously described for other Pt(II) complexes.[32] The PtL^1Cl complex was readily converted into PtL^1NCS upon treatment with sodium thiocyanate in methanol/dichloromethane at room temperature.[13] The new proligands HL^1 and HL^2, and their Pt(II) derivatives were fully characterized by elemental analysis, mass spectrometry and NMR spectroscopy.

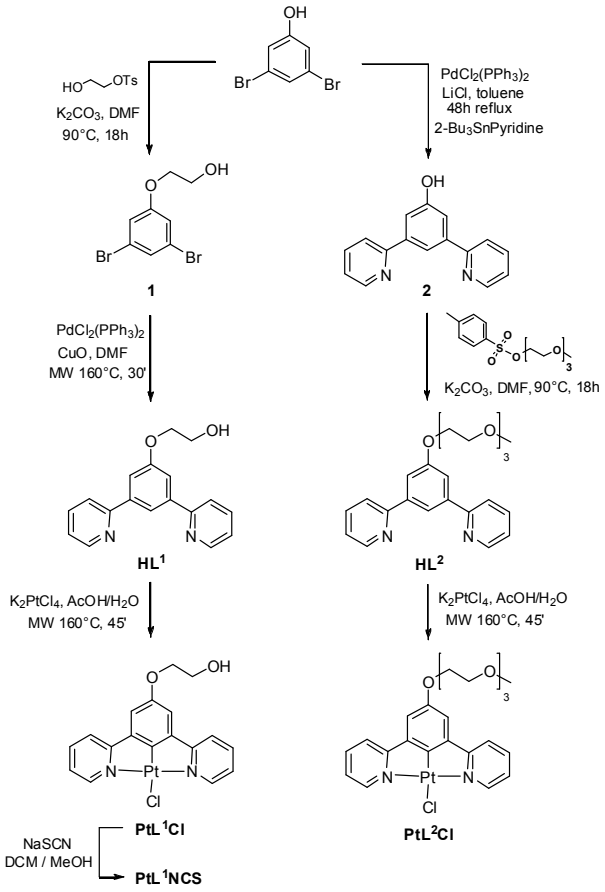

Scheme 1. Synthetic pathway for the preparation of the reported platinum complexes.

Photophysical properties

In order to evaluate the potential of the novel neutral platinum complexes as luminescent labels for bio-imaging purposes, we have investigated their photophysical properties in solution. For all three compounds, the absorption and emission spectra are displayed in Figure 2 and recorded for sample concentration of 1.0×10^{-5} M in dichloromethane solution at room temperature, while the corresponding photophysical data are listed in Table 1.

Table 1. Most meaningful photophysical data of the complex **PtL^{1}Cl**, **PtL^{1}NCS** and **PtL^{2}Cl** in dilute CH_2Cl_2 solution at room temperature and in CH_2Cl_2:MeOH 1:3 glassy matrix at 77 K.

Complex	λ_{abs} [nm] ($\varepsilon\times10^{-3}$/[$M^{-1}cm^{-1}$])	λ_{em} [nm]	PLQY	τ [μs]	PLQY	τ [μs]	λ_{em} [nm]	τ [μs]
		air-equilibrated			*degassed*		*77 K*	
PtL^{1}Cl	293 (23), 326 sh (6), 378 (6), 438 (7)	542, 574(sh)	0.01	0.27	0.49	12.4	529, 568, 610(sh)	13.6
PtL^{1}NCS	293 (13), 332 sh (2), 374 (2), 430 (4)	540, 571(sh)	0.02	0.39	0.46	11.8	530, 571, 615	13.6 [a] 13.1 (20%) 3.8 (80%) [b]
PtL^{2}Cl	293 (20), 361 sh (3), 378 (5), 436 (6)	546, 574(sh),	0.02	0.28	0.66	12.1	531, 572, 615	14.4

[a] recorded at λ_{em} = 520 nm.
[b] recorded at λ_{em} = 625 nm.
The abbreviation "sh" denotes a shoulder

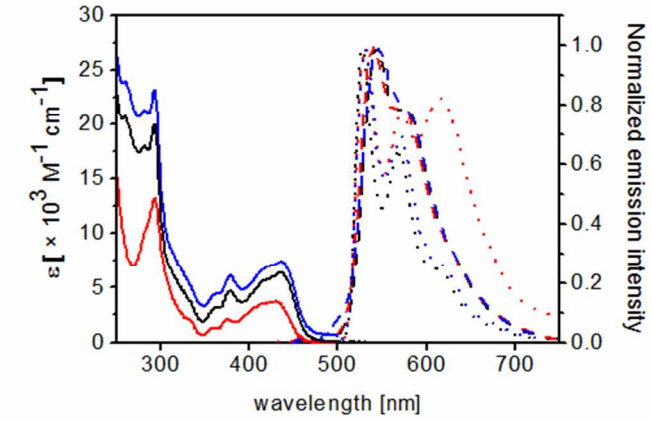

Figure 2. Absorption (solid traces) and emission spectra (dashed traces) in CH_2Cl_2 at room temperature and emission spectra in CH_2Cl_2:MeOH 1:3 glassy matrix at 77 K (dotted traces) for the complex PtL^{1}Cl (black traces), PtL^{1}NCS (red traces) and PtL^{2}Cl (blue traces). Emission spectra were recorded upon λ_{exc} = 300 nm.

The CH_2Cl_2 solutions of the complexes (1.0×10^{-5} M) showed electronic absorption features into the UV-visible range typical of this class of compounds bearing a 1,3-di(2-pyridyl-benzene), N^C^N, chromophoric ligand as firstly reported by Williams and co-workers.[33] In the region between 250–300 nm, the absorption spectra is characterized by rather intense (ε = 1.3–2.3×10^4 M^{-1} cm^{-1}) electronic transitions assigned to singlet-manifold spin-allowed ligand centered (^{1}LC) excitation processes mainly involving the 1,3-di(2-pyridyl-benzene) cyclometalating ligand.[33] At lower energy (λ_{abs} = 370–440 nm), the samples show much weaker bands with molar excition coefficient in the range of $4–6\times10^3$ M^{-1} cm^{-1} and attributed to mixed transitions possessing ^{1}LC and metal-to-ligand charge transfer, ^{1}MLCT, character.[33]

Upon excitation at 300 nm, dilute CH_2Cl_2 solutions of all the three investigated complexes displayed bright structured luminescence in the green-yellow region of the visible electromagnetic spectrum. The emission energies are only slightly dependent on the ancillary ligand (λ_{em} = 542, 540 and 546 nm for derivative **PtL^{1}Cl**, **PtL^{1}NCS** and **PtL^{2}Cl**, respectively), and the luminescence of the complexes displays vibronic progression attributable to the intraligand modes, on the basis of extensive studies reported for closely-related N^C^N platinum complexes.[34,35]

While the emission profile does not appear to be dependent on the presence of the quenching dioxygen molecules, upon degassing procedure all the samples showed a much more intense emission with PLQY that reached values as high as 0.49, 0.46 and 0.66 for **PtL^{1}Cl**, **PtL^{1}NCS** and **PtL^{2}Cl**, respectively, *versus* 0.01–0.02 obtained for the corresponding air-equilibrated samples. Such enhancement of the PLQY on going from air-equilibrated to degassed solution is typical of luminescent compounds emitting from a triplet excited state and is accompanied by a concomitant prolongation of the excited-state lifetime, being as long as 12.4, 11.8 and 12.1 μs for **PtL^{1}Cl**, **PtL^{1}NCS** and **PtL^{2}Cl**, respectively (see Table 1). The high emission efficiency can be associated to the rigidity of the terdentate cyclometalated ligand, which reduces the molecular distorsions of the excited states, thus disfavouring the pathway of nonradiative decays,[35,36] and the strong ligand field of the tridentate chelate increases the energy of the metal centered (MC) d–d excited states, that are common deactivation paths for the luminescent state.

In order to further investigate the nature of the radiative transition responsible for such bright emission, we performed photoluminescence studies of the complexes in CH_2Cl_2:MeOH 1:3 glassy matrix at low (77 K) temperature (see Figure 2 and Table 1). Upon lowering the temperature and rigidification of the environment, the glassy samples displayed a more structured and slighty hypsochromically shifted (ca. 450 cm^{-1}) emission spectra with a parallel, yet minor, prolongation of the excited state lifetime up to 13.6–14.4 μs. These observations evidence the weak metal-to-ligand charge transfer character of the lowest ^{3}LC excited state.

Noteworthy, while samples of the two chloro-containing derivatives do not show any additional band in the spectra recorded at 77 K, for the derivative bearing the SCN^- as the ancillary ligand the emission spectrum clearly displays a lower-energy lying band centered at *ca.* 625 nm, indicating the presence of closely-interacting platinum complexes. The excitation spectra recorded at both λ_{em} = 520 and 625 nm (see Figure S1 of the ESI), are almost identical to the absorption spectra recorded in dilute CH_2Cl_2 solution. We can therefore conclude that, since no ground state aggregation is present, the lower-energy band is due to an excited state arising from the formation of excimers, as also reported by us for other related (N^C^N)PtNCS derivatives.[13] Furthermore, for both complex

PtL^{1}Cl and **PtL^{2}Cl** the luminescent excited state decay follows a monoexponential kinetics with τ = 13.6–14.4 μs. On the other hand, for complex **PtL^{1}NCS** while a similar lifetime (τ = 13.6 μs) was measured monitoring the emission at λ_{em} = 520 nm, a bi-exponential decay was recorded at λ_{em} = 625 nm, being τ_1 = 13.1 μs (20%) and τ_2 = 3.8 μs (80%). Such shorter component is ascribed to the emission arising to excimeric species (see Table 1).

Closer look at the molecular structure of the complex **PtL^{2}Cl** reveals its amphiphilic nature, where the tridentate "platinum-Cl" core is the hydrophobic head and the triethylen glycol chain is the hydrophilic tail. In order to further investigate the photophysical properties of **PtL^{2}Cl** and the possibility to establish metallophilic Pt···Pt and π–π stacking interactions, with subsequent modulation of both excitation and emission properties,[19-20,27] aggregation studies were performed in air-equilibrated dioxane–water mixture at different ratio ranging from pure dioxane to dioxane–water 1:4. During these experiments, the concentration of the amphiphilic complex **PtL^{2}Cl** was kept constant (5×10^{-5} M), and it is identical to that used in the bio-imaging experiments (see below). In this way it is possible to evaluate the sole effect of the polarity of the media and the solvent/non-solvent ratio on the photophysical properties. Indeed, in these conditions, the dioxane is expected to play the role of a good solubilizing solvent for the emissive complex, while the water acts as the non-solvent. The absorption and emission spectra of the five investigated solutions are displayed in Figures 3 and 4, respectively, and the photohysical data summarized in Table S1 of the ESI.

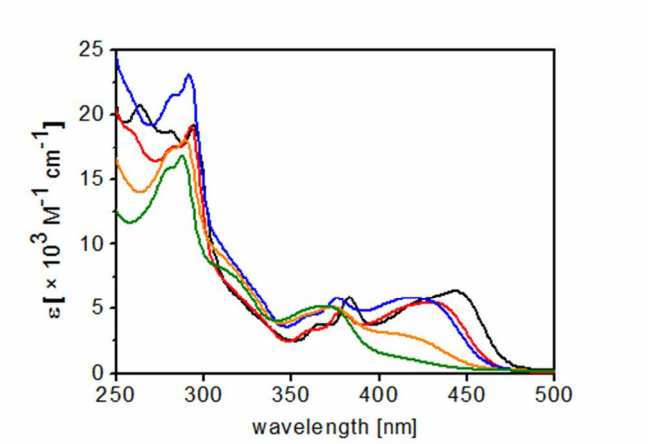

Figure 3. Absorption spectra of complex **PtL^{2}Cl** at concentration of 5×10^{-5} M in air-equilibrated dioxane–water mixture at different ratio: 100:0 (black trace), 80:20 (red trace), 60:40 (blue trace), 40:60 (orange trace) and 20:80 (green trace).

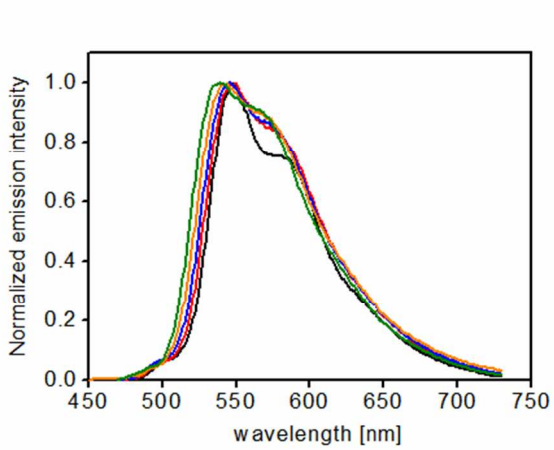

Figure 4. Emission spectra of complex **PtL^{2}Cl** at concentration of 5×10^{-5} M in air-equilibrated dioxane–water mixture at different ratio: 100:0 (black trace), solution 1, 80:20 (red trace), 60:40 (blue trace), 40:60 (orange trace), 20:80 (green trace). The samples were excited at λ_{exc} = 400 nm (100:0, 80:20, 60:40) and at λ_{exc} = 420 nm (40:60 and 20:80).

Upon increasing the water content, a steady negative solvatochromic shift and decrease of the intensity of the lowest-lying band is clearly visible, which is in line with the attribution of the CT character of the electronic excitation in such class of compounds.[33,37] Also, such finding implies the sizeable decrease of the excited-state electric dipole moment respect to that of the ground-state.[37] A similar hypsochromic shift upon increase of solvent polarity has been observed in the photoluminescence spectra, indicating a significant variation, and in particular a decrease, of the excited state dipole moment. Nonetheless, despite the amphiphilic nature of the molecules, the rather low emission intensity observed (PLQY = 1–2%) at any dioxane-water content rules out the presence of supramolecular organized structures in which the hydrophobic platinum cores are arranged in such a way to protect themselves from surrounding quenching dioxygen and water molecules.[38] Furthemore, the absence of lower-lying bands in both absorption and emission spectra indicates the lack of any ground-state metallophilic Pt···Pt and π–π stacking interactions. On the other hand, time-resolved emission decays revealed bi-exponential kinetics with a shorter (τ_1 = 4–5 ns) and a longer component (τ_2 of few hundreds of ns), where the relative weight of the former increases upon increasing the water content of the mixture (see Table S1 of the ESI). Although such very short decay would point towards the substitution of the ancillary Cl^- ligand with a water molecule at first glace, we believe that it should not be the case here due to the fact that the compound is prepared in boiling acetic acid – water mixture. Yet, such short lifetime component could rather unravel the establishment of specific solvent-solute interactions (*e.g.*, H-bonding between H_2O and chlorine ligand ancillary) which might favour efficient deactivation processes *via* radiationless pathways.

Bioimaging studies

In order to investigate the internalization and bio-imaging properties of the novel Pt(II) complexes as molecular probes, cellular uptake experiments were carried out on living *Human cervical carcinoma*, HeLa, cell line at normal biological

condition (37°C, 5% CO_2) by varying the staining solution in terms of platinum complex concentration and buffer used. The results of the internalization experiments upon incubation of HeLa cells with the three reported complexes, namely **PtL^{1}Cl**, **PtL^{1}NCS** and **PtL^{2}Cl**, at concentration of 50 μM in less than 1% DMSO/phosphate buffer saline (PBS) are displayed in Figure 5.

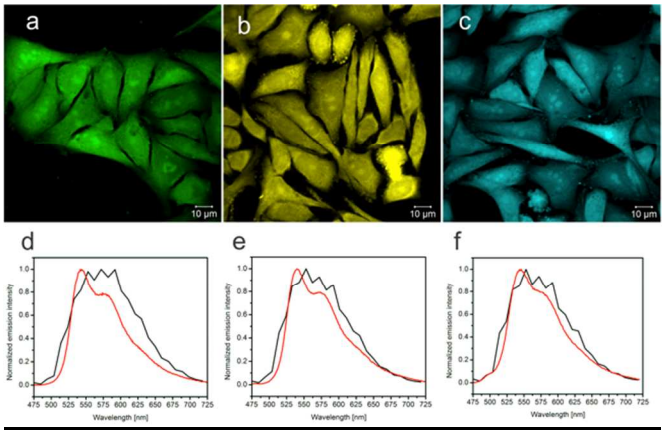

Figure 5. Fluorescence confocal microscopy images of the internalization of three different platinum complexes at 50 μM into HeLa cells with <1% DMSO/PBS as the incubating media. a) **PtL^{1}Cl**, b) **PtL^{1}NCS**, and c) **PtL^{2}Cl**. The emission spectra recorded from different cellular regions are displayed (λ_{exc} = 405 nm, black traces) for d) **PtL^{1}Cl**, e) **PtL^{1}NCS**, and f) **PtL^{2}Cl**, and compared to the corresponding emission recorded in dilute CH_2Cl_2 (λ_{exc} = 300 nm, red traces).

Under these conditions, as it can be seen by analyzing the fluorescence confocal images, staining solutions containing each of the three compounds show rapid (within 10 minutes) internalization of the platinum complex into HeLa cells (Figure 5). In order to gain deeper insights into the chemical nature (either monomeric compound or aggregated species) of the emissive species responsible for the photoluminescence of the stained cells, we recorded photoluminescence spectra of cellular compartments upon platinum complex uptake and the results are shown in Figure 5d–f (black traces). For all the investigated complexes, an intense and broad emission band has been observed. The recorded emission spectra are centered at around 560 nm for all the three complexes, namely **PtL^{1}Cl**, **PtL^{1}NCS** and **PtL^{2}Cl**.

Furthermore, comparison of the emission profile obtained from living cells with the photoluminescence spectra recorded in dilute dichloromethane solution (Figure 5d–f, red traces) shows negligible difference, confirming the similar nature of the emitting excited state for the two compared conditions and ruling out an emission arising from aggregated or interacting complexes through Pt···Pt or π–π interactions (see also photophysical aggregation study).

In order to confirm the effective internalization of the platinum complexes inside the cells, *z*-stack experiments were also carried out on cells stained with PhalloidinAlexa Fluor® 647, as the *f*-actin and membrane label, by means of confocal microscopy. The obtained results, including the orthogonal views, are shown in Figure 6a for complex **PtL^{1}Cl**, and undoubdtely confirm that cellular uptake of the novel platinum derivatives took place. The results of the *z*-stack experiments for **PtL^{1}NCS** and **PtL^{2}Cl**, are displayed in Figure S2a and S3a of the ESI, respectively.

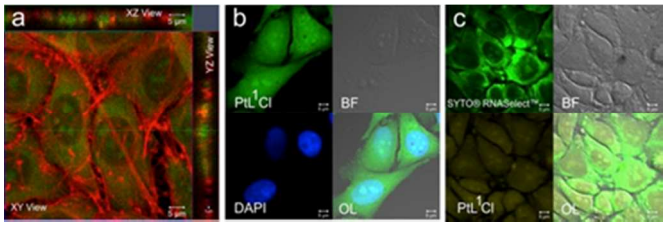

Figure 6. Fluorescence confocal microscopy images of the distribution of **PtL^{1}Cl** (50 μM in less than 1% DMSO containing PBS) inside HeLa cells and co-localization experiments showing the presence of compound **PtL^{1}Cl** inside the cell nucleus, nucleoli, and cytoplasmic parts of the cell. (a) Orthogonal views of the image showing **PtL^{1}Cl** signal (green) coming from inside cytoplasmic and nuclear region of the cells. The cells are stained with Phalloidin Alexa Fluor® 647 (red). (b) **PtL^{1}Cl**, bright-field (BF) image of HeLa cells, DAPI staining of nucleus, and overlay (OL) of three panels (c) SYTO® RNASelect™ green stains RNA inside cells including nucleoli; BF image, **PtL^{1}Cl**, and overlay of three panels. The excitation wavelength for DAPI and **PtL^{1}Cl** was 405 nm, while SYTO® RNASelect™ and Phalloidin Alexa Fluor® 647 were excited at 488 and 633 nm, respectively.

Upon internalization, the complexes are distributed throughout cellular cytoplasmic compartments and, more interestingly, they are also present into the nuclear region, independently from their molecular structure or their more hydrophobic/hydrophilic nature.

To further investigate the uptake and accumulation of the complexes (50 μM <1% DMSO/PBS), co-localization experiments were carried out by using 4',6-diamidino-2-phenylindole-6-carboxamidine (DAPI), SYTO® RNASelect™ and Alexa Fluor® 647 Phalloidin as the nucleus, the nucleoli and the *f*-actin/membrane staining agent, respectively. The corresponding microscopy images obtained upon 20 minutes incubation are displayed in Figure 6b-c for complex **PtL^{1}Cl** and S2b-c–S3b-c of the ESI for derivative **PtL^{1}NCS** and **PtL^{2}Cl**, respectively. Such co-staining experiments clearly confirmed the ability of the three reported platinum complexes to cross the nuclear membrane and localize inside the nuclear region as well. Indeed, a rather good overlap (overlap coefficient = 0.9) can be also observed when signal arising from the SYTO® RNASelect™ and platinum complexes are compared, confirming the presence of the complex inside nucleoli as previously reported using N^N^N tridentate platinum complexes,[19,20] and observed for a related N^C^N derivative.[22,23] Noteworthy, the presence of an SCN^- group as the ancillary ligand instead of the Cl^- (**PtL^{1}Cl** *vs* **PtL^{1}NCS**) as well as the introduction of a more hydrophilic triethylenglycol chain onto the cyclometalating phenyl ring (**PtL^{1}Cl** *vs* **PtL^{2}Cl**) do not significantly affect the uptake behaviour in terms of cellular sub-localization, as shown in Figure 6 and Figure S2–3 of the ESI.

In order to monitor real-time event under normal cellular condition, an ideal bio-imaging probe should not influence, strongly interact or alter the correct cellular functioning and bio-chemical processes. Thus, luminescent molecules used as staining should preferentially be present at a concentration as low as possible. To this end, we performed concentration effect and kinetics studies in living HeLa cells. By lowering the

concentration of the staining platinum complexes down to 5 μM in <1% DMSO/PBS as the incubating media, cellular uptake was found to be very rapid as well, and the emission from the platinum complexes inside the cells appeared just one minute after addition of the platinum(II) complex onto the cells. The staining pattern of the cytoplasmatic and nuclear region was found to increase over the time reaching a plateau after 10 minutes of incubation, as shown in Figure 7 and Figure S4–5 of the ESI for complex **PtL^{1}Cl**, **PtL^{1}NCS** and **PtL^{2}Cl**, respectively. Such rapid internatization kinetics might be due to an efficient diffusion-controlled uptake mechanism, even though a parallel energy-driven mechanism can not be ruled out at this stage.

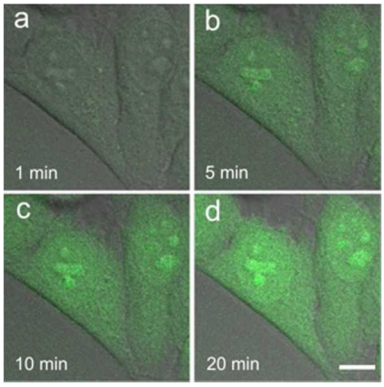

Figure 7. Confocal images of the kinetics experiments of HeLa cells incubated with **PtL^{1}Cl** at concentration 5 μM in <1% DMSO/PBS at different incubation time: (a) 1 minute, (b) 5 minutes, (c) 10 minutes, and (d) 20 minutes, showing the fast internalization of the compound. The samples were excited at λ_{exc} = 405 nm. Scale bar is 10 μm.

By comparing the kinetic experiments performed at 5 μM of the platinum complexes, we were able to evidence the effect exerted by both the ancillary ligand and the longer triethylenglycol chain. Indeed, while the uptake of complex **PtL^{1}Cl** by living HeLa cells was found to be the fastest amongst the three different platinum derivatives employed, introduction of a longer triethylen glycol chain slightly slowed down the kinetics, as demonstrated by the lower intensity of the signal recorded with the confocal microscope under identical excitation power. Such effect can be most likely ascribed to the larger molecular size of the **PtL^{2}Cl** when compared to **PtL^{1}Cl**, since the longer polar (*i.e.*, triethylenglycol) chain is expected to impart a more amphiphilic character to the complex, thus helping to cross the lipophilic cellular membranes.[20,29,30]

Moreover, it has been found that the derivative bearing the NCS ligand, namely **PtL^{1}NCS,** shows the slowest cellular internalization kinetics. Indeed, for this complex the signal observed after one minute of incubation was almost negligible and photoluminescence started to appear after five minutes, yet with low intensity. Afterwards, an internalization pattern somehow similar to that obtained for staining solution at 50 μM started to appear for all the three platinum derivatives (see Figure 7 and Figure S4–5 of the ESI, box b–d).

Since the incubation media can play an important role for the uptake of platinum complexes and not always the change from PBS to cell culture media leads to the same results,[20] we have also investigated the behaviour of the compounds using the commercial DMEM. The switch from PBS to DMEM, as culture media, gave similar uptake results for the three investigated complexes, as shown in Figure S6 of the ESI for complex **PtL^{2}Cl**, as an example.

Finally, it is worth noticing that even after 30 minutes of incubation the cell possess an healthy appearance and no evident sign of apoptosis were observed during the imaging experiments. This observation indicates a negligible degree of toxicity of the internalized compounds inside the cells, which is quite surprising since as already mentioned the compounds are in the nucleus. To further quantify such finding, viability tests were performed by means of the CASY® equipment in order to evaluate the cytotoxiticy and the results are shown in Figure 8.

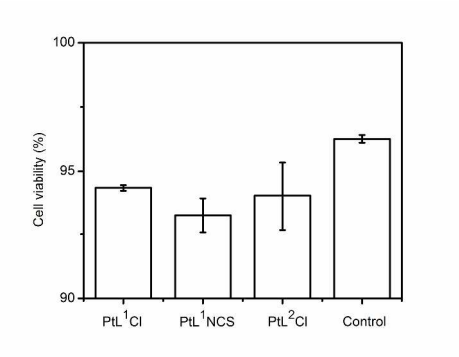

Figure 8. Cellular viability studies after 30 minutes incubation with different complexes at concentration of 50 μM in <1% DMSO containing culture media.

Interestingly, the number of viable cells after 30 minutes incubation of the different complexes, a time much longer than the one used for the imaging experiments, are found to be close to the control experiments, strongly indicating the low cytotoxicity of the complexes and their suitability as efficient phosphorescent probes to be used in bio-imaging application.

Conclusions

In this work we prepared and fully characterized three new platinum(II) complexes bearing cyclometallated di(2-pyridyl)-benzene substituted with ethylenglycol moieties of various lengths, as luminescent bio-labels. We have performed a systematic study of their bio-imaging and cytotoxicity features not only varying the molecular hydrophobic/hydrophilic ratio, by using different ethylenglycol substituents and the ancillary ligand, but also changing the incubating media and the staining concentration. Remarkably, all complexes are characterized by a high cell permeability, low cytotoxicity and an internalization kinetics that depends on both the length of the ethylenglycol chain and the ancillary ligand. The uptake of complex **PtL^{1}Cl** by living *Human cervical carcinoma*, HeLa, cells was found to be extremely rapid (one minute only) and the fastest amongst the three different platinum derivatives employed, probably due to its smaller molecular size.

Our results confirm the ability of terdentate N^C^N platinum complexes to cross the nuclear membrane and localize inside the nuclear region as well. They also suggest that the introduction of a more hydrophilic triethylenglycol chain onto the cyclometallating phenyl ring does not significantly affect the uptake behavior in terms of cellular sub-localization. Further studies are needed to gain a better understanding of the

relationship between the chemical structure of the coordination sphere of platinum(II) and the localization site inside the cell.
In any case, it is worth pointing out that the introduction of oligo-ethylenglycol chains, which allow a very low cytotoxicity, could be a tool to increase not only the aqueous solubility but also the biocompatibility of highly luminescent Pt(II) complexes families for bio-imaging application.

Acknowledgements

In Italy, this work was supported by the Ministero dell'Istruzione, dell'Università e della Ricerca (FIRB 2004:RBPR05JH2P and PRIN 2008:2008FZK5AC_002).
L.D.C., M.M., F.F., and D.S. kindly acknowledge Université de Strasbourg, CNRS, the Région Alsace, the Communauté Urbaine de Strasbourg, the Département du Bas-Rhin, and the Ministère de l'Enseignement Supérieur de la Recherche (MESR) for funding the purchase of the confocal microscope.
ERC grant n. 2009-247365, is acknowledge for financial support. L.D.C. is also grateful to AXA Research funds.

Notes and references

[a] Dipartimento di Chimica dell'Università degli Studi di Milano, UdR-INSTM.
[b] ISIS & icFRC, Université de Strasbourg & CNRS, 8 rue Gaspard Monge, 67000 Strasbourg, France.
[c] ISTM-CNR, via Golgi 19, I-20133, Milano, Italy.
[d] University of Strasbourg Institute for Advanced Study (USIAS), 5 allée du Général Rouvillois, 67083 Strasbourg, France.
# All these authors have contributed equally to the work.

Electronic Supplementary Information (ESI) available: additional photophysical data, spectra and bio-imaging studies. See DOI: 10.1039/b000000x/

1 T. Krigas, B. Rosemberg, L. Van Camp, *Nature*, 1965, **205**, 698.
2 B. Rosenberg, *Plat. Met. Rev.,* 1971, **15***,* 42.
3 Z. Guo, P. J. Sadler, *Adv. Inorg. Chem.,* 2000, **49***,* 183.
4 S. J. Lippard, T. C. Johnstone, J. J. Wilson, *Inorg. Chem*., 2013, **52**, 12234.
5 Y.-R. Zheng, K. Suntharalingam, T. C. Johnstone, H. Yoo, W. Lin, J. G. Brooks, S. Lippard *J. Am Chem. Soc.,* 2014, **136**, 8790.
6 J.A.G. Williams, S. Develay, D.L. Rochester, L. Murphy, *Coord. Chem. Rev.*, 2008, **252**, 2596.
7 C. Cebrián, M. Mauro, D. Kourkoulos, P. Mercandelli, D. Hertel, K. Meerholz, C. A. Strassert, L. De Cola, *Adv. Mater.,* 2013, **25**, 437.
8 M. Mauro, A. Aliprandi, C. Cebrian, D. Wang, C. Kübel, L. De Cola, *Chem. Comm*., 2014, **50**, 7269.
9 Y. Tanaka, K. M.-C. Wong, V. W.-W. Yam, *Angew. Chem. Int. Ed*. 2013, **52**, 14117.
10 C. Po, Z. Ke, A.Y.-Y. Tam, H.-F. Chow, V. W.-W. Yam, *Chem. A. Eur. J.* 2013, **19,** 15735.
11 S. J. Farley, D. L. Rochester, A. L. Thompson, J. A. K. Howard, J. A. G. Williams, *Inorg. Chem.*, 2005, **44**, 9690.
12 E. Rossi, L. Murphy, P. L. Brothwood, A. Colombo, C. Dragonetti, D. Roberto, R. Ugo, M. Cocchi, J. A. G. Williams, *J. Mat. Chem.*, 2011 **21**, 15501.
13 E. Rossi, A. Colombo, C. Dragonetti, D. Roberto, F. Demartin, M. Cocchi, P. Brulatti, V. Fattori, J. A. G. Williams, *Chem. Comm.,* 2012, **48**, 3182.
14 F. Nisic, A. Colombo, C. Dragonetti, D. Roberto, A. Valore, J. M. Malicka, M. Cocchi, G. R. Freeman, J. A. G. Williams, *J. Mat. Chem. C*, 2014, **2**, 1791.
15 A. Valore, A. Colombo, C. Dragonetti, S. Righetto, D. Roberto, R. Ugo, F. De Angelis, S. Fantacci, *Chem. Comm.,* 2010, **46**, 2414.
16 A. Colombo, C. Dragonetti, D. Marinotto, S. Righetto, D. Roberto, S. Tavazzi, M. Escadeillas, V. Guerchais, H. Le Bozec, A. Boucekkine, C. Latouche, *Organomet.,* 2013, **32,** 3890.
17 E. Rossi, A. Colombo, C. Dragonetti, S. Righetto, D. Roberto, R. Ugo, A. Valore, J. A. G. Williams, M. G. Lobello, F. De Angelis, S. Fantacci, I. Ledoux-Rak, A. Singh, J. Zyss, *Chem.-A Europ. J.,* 2013**,** **19**, 9875.
18 J. Boixel, V. Guerchais, H. Le Bozec, D. Jacquemin, A. Amar, A. Boucekkine, A. Colombo, C. Dragonetti, D. Marinotto, D. Roberto, S. Righetto, R. De Angelis, *J. Am. Chem. Soc.,* 2014, **136**, 5367.
19 D. Septiadi, A. Aliprandi, M. Mauro, L. De Cola, *RSC Adv.* 2014, **4**, 25709.
20 M. Mauro, A. Aliprandi, D. Septiadi, N.S. Kehr, L. De Cola, *Chem. Soc. Rev.,* 2014, **43**, 4144.
21 E. Baggaley, J. A. Weinstein, J. A. G. Williams, *Coord. Chem. Rev.,* 2012, **256**, 1762.
22 S.W. Botchway, M. Charnley, J. W. Haycock, A. W. Parker, D. L. Rochester, J. A. G. Williams, *Proc. Nat. Acad. Sci. USA*, 2008, **105**, 16071.
23 E. Baggaley, S. W. Botchway, J. W. Haycock, H. Morris, I. V. Sazanovich, J. A. G. Williams, J. A. Weinstein, *Chem. Sci.,* 2014, **5**, 879.
24 R. Y. Tsien, *Angew. Chem. Int. Ed*., 2009, **48**, 5612.
25 R. D. Moriarty, A. Martin, K. Adamson, E. O'Reilly, P. Mollard, R. J. Forster and T. E. Keyes, *J. Microsc*., 2014, **253**, 204.
26 Z. Guo, S. Park, J. Yoon, I. Shin, *Chem. Soc. Rev*., 2014, **43**, 16.
27 C. Y.-S. Chung, S. P.-Y. Li, M.-W. Louie, K. K.-W. Lo, V. W.-W. Yam, *Chem. Sci*., 2013, **4,** 2453.
28 V. Fernández-Moreira, F. L. Thorp-Greenwood, M. P. Coogan, *Chem. Commun*, 2010, **46**, 186.
29 Q. Zhao, C. Huang, F. Li, *Chem. Soc. Rev.*, 2011, **40**, 2508.
30 A.W.-T. Choi, M.-W. Louie, S. P.-Y. Li, H.-W. Liu, B. T.-N. Chang, T.C.-Y. Lam, A. C.-C. Lin, S.-H. Cheng, K. K.-W. Lo, *Inorg. Chem*., 2012, **5**1, 13289.
31 J.S. Bradshaw, K. E. Krakowiak, G. C. LindH, R. M. Izatt *Tetrahedron,* 1987, **43**, 4271.
32 Z. Wang, E. Turner, V. Mahoney, S. Madakuni, T. Groy, J. Li, *Inorg. Chem.*, 2010, **49**, 11276.
33 J.A.G. Williams, A. Beeby, E. S. Davies, J. A. Weinstein, C. Wilson, *Inorg. Chem*., 2003, **42**, 8609.
34 H. Yersin, W. Humbs, J. Strasser, *Top. Cur. Chem.*, 1997, **191**, 153.
35 A.F. Rausch, L. Murphy, J.A.G. Williams, H. Yersin, *Inorg. Chem.,* 2012, **51**, 312.
36 G.S.-M. Tong, C.-M. Che, *Chem.–Eur. J*. 2009, **15**, 7225.
37 D.M. Manuta, A. J. Lees, *Inorg. Chem.* 1986, **25**, 3212.
38 M. Mauro, G. De Paoli, M. Otter, D. Donghi, G. D'Alfonso, L. De Cola, *Dalton Trans.* 2011, **40**, 12106.

Table of Content

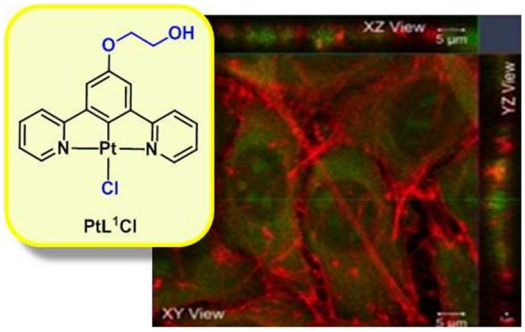

The reported cyclometallated Pt (II) complexes are characterized by a high cell permeability and low cytotoxicity. In particular PtL^1Cl shows a very fast internalization kinetics.

Graphycal abstract

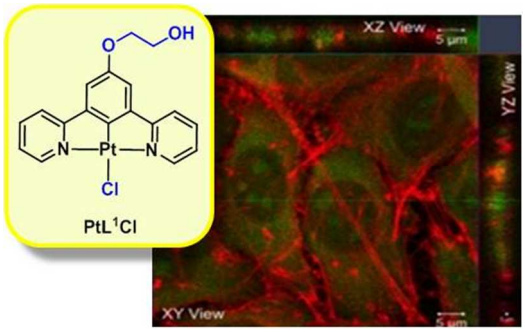

The reported cyclometallated Pt (II) complexes are characterized by a high cell permeability and low cytotoxicity. In particular PtL^1Cl shows a very fast internalization kinetics.